# Generation and Propagation of vibrations induced by high-speed railways

João Manso

Abstract

In the years to come, Portugal has several challenges to overcome and one is to try to modernize its train network. Among other issues, vibrations are a major concern, specially due to high speed traffic. Therefore, a two-dimensional model has been designed, considering some hypotheses (straight tracks, constant longitudinal geometric and mechanic characteristics), to predict both generation and propagation of those vibrations.

Although the phenomena is three-dimensional, a two-dimensional model is less time consuming and easier to implement, but there are some aspects to take into consideration, like, for example, geometrical soil damping. To overcome and comparing them to *in situ* values, a method that corrects the results has been proposed.

To compare the *in situ* results with the results from the model, there are several filters that could be used to reduce random noise from a signal, while retaining a sharp step response, but, for time domain analysis, moving average filters are the premier filter to use.

Both the train himself (weights and geometry) and track irregularities, are the most relevant vibration sources from high speed traffic. So, taking into consideration the train weight, the distances between axles and a stochastic process to model the rail roughness, those actions could be predicted.

There are some conclusions, in this work, that should me mentioned referring to two-dimensional model results. One is that they don't consider geometrical damping correctly, so, surface wave vibrations should be corrected by a factor.

**Keywords**

High-speed trains, axle loads, track irregularities, vibrations, geometric and material damping, two-dimension numerical model

## Introduction

The development of tracks of high-speed trains has increased in the last decades in countries of Europe, North America and Asia. Trains are now able to achieve velocities of 300 km/h and higher, so its consequences to people and structures became a major concern. Numerical models and *in situ* and laboratory tests can be made to study some of those consequences and to test new methods to decrease them.

This work is divided in three parts, it starts with a study of generation of vibrations, including the consideration of both the axles' loads and the track irregularities.

The second part consists in the study of the propagation of vibrations in the soil, since the source until a finite distance from it. The existing waves are identified and characterized, in terms of direction, velocity of propagation and type of damping.

In order to test the achievements obtained is this work, a two-dimensional model has been designed and the results are shown and compared, using several analysis.

## Generation of vibrations

According to Hall (2002), there are uncountable factors that influence the characteristics of vibrations, induced by high-speed railways, such as the response of the structure and its foundations, generating waves with frequencies in the range 0 to 2000 Hz (Table 1) with different sources (Nielsen, 2008):

- response of the structure to train loads, at different velocities;
- vibrations due to the interface wheel-track;
- discontinuity of the rail;
- differences between foundations and support through the track.

*Table 1 - Frequencies generated from different sources of vibration*

| Sources of vibration | Frequencies |
|---|---|
| Ballast and foundation | 0,7 to 5 Hz |
| Bogie | 5 to 20 Hz |
| Wheel | 20 to 100 Hz |
| Interface wheel-rail | 0,1 to 1 kHz |

In this work, two types of sources of vibration have been studied: the axle loads and the irregularities in train wheels and rails, which will be referred in the following paragraphs.

### *Axles loads*

Considering only the variable velocity, it is possible to have two types of answers: one at low speed and another at high speed. The first example it's usually designated as quasi-static analysis, meaning that vibrations are only due to moving axle loads. However, when velocity increases, dynamics loads tend to become even more important than the static ones (Sheng et al., 2003).

In this analysis, an important value is the critical velocity (related to the resonance phenomenon), which, according to Kenney (1954) and considering the Winkler beam with no damping, can be obtained by:

$$v_{cr} = \sqrt[4]{\frac{4kEI}{m^2}} \qquad \textit{Eq. 1}$$

where $k$ is the equivalent rigidity of the Winkler beam foundation, $EI$ stands for the bending rigidity of the

beam and *m* represents the beam's mass by unit length.

For velocities equal to the critical one, the resonance phenomenon occurs, producing infinite deformations in the Winkler beam. However, for velocities below the critical one, the load curve tend to be symmetric, changing its width depending on the value of the velocity.

The quasi-static loads, for velocities below the critical one with no damping, can be determined using:

$$F(s)=\frac{F_e}{2\mathrm{L}}e^{-|\frac{s}{L}|}(\cos(|\frac{s}{L}|)+\sin(|\frac{s}{L}|)) \qquad \textit{Eq. 2}$$

where *F(s)* is the load distribution of a single axle in a given referential, $F_e$ stands for the axle load, *L* represents the characteristic length and *s* is the value of a moving referential with origin in the axle position. In Eq. 2 the critical velocity is not considered, so it is important to verify if the velocity is smaller than the critical one, before applying the equation.

It is possible to change from the static referential, *x*, to the moving referential, *s*, by simple applying the relation:

$$s=\frac{1}{L}(x-v_0 t) \qquad \textit{Eq. 3}$$

where $v_0$ stands for the train velocity and *t* represents the time. Therefore, the load distribution, related to time and the static referential, comes:

$$F(x,t)=\frac{F_e}{2\mathrm{L}}e^{-|\frac{x-v_0 t}{L^2}|}(\cos(|\frac{x-v_0 t}{L^2}|)+\sin(|\frac{x-v_0 t}{L^2}|)) \qquad \textit{Eq. 4}$$

Finally, it is possible to obtain the characteristic length by calculate the next expression:

$$L=\sqrt[4]{\frac{4\mathrm{EI}}{k}} \qquad \textit{Eq. 5}$$

Having several load distributions for each single axle, it is only needed to sum all the axles of the train:

$$F=\sum_{i=1}^{i=n}F_i \qquad \textit{Eq. 6}$$

## *Irregularities*

Like it has been told, there are several excitation mechanisms, when referring to vibrations induced by high-speed trains. Other mechanisms of great importance, in addition to train loads, are the track and the wheels irregularities (Gupta et al., 2007 and Esveld, 2001).

The existence of those irregularities can be imposed to the numerical model in terms of displacements using a linear method, depending on the wave length, $\lambda$.

To obtain the load, due to those irregularities, firstly we should consider a contact force between the rail and the train wheel, relating to the frequency, $\hat{g}(\omega)$:

$$[K^{v}(\omega)+K^{tr}(\omega)]\,\hat{g}(\omega)=\hat{u}_{w/r}(\omega) \qquad \textit{Eq. 7}$$

where $\hat{u}_{\omega/r}$ is the track/wheel irregularity, $K_v(\omega)$ represents the vehicle rigidity matrix and the $K_{tr}(\omega)$ stands for the track rigidity matrix. Using a power density spectrum, $\hat{G}'_{\omega/r}(n_y)$, is possible to define the roughness of the track, $\hat{u}_{\omega/r}(y)$, in terms of the inverse of the wave length, $n_y=f/v=1/\lambda_y$:

$$G'_{w/r}(n_y)=\frac{A' n_{y2}^2 (n_y^2+n_{y1}^2)}{n_y^4 (n_y^2+n_{y2}^2)} \qquad \textit{Eq. 8}$$

By calculating the ratio between Eq. 8 and $2\pi$, we obtain the spectrum in terms if the wave number, $k_y$:

$$G_{w/r}(k_y)=\frac{G'_{w/r}(n_y)}{2\pi} \qquad \textit{Eq. 9}$$

The Federal Railroad Administration (FRA) defined 6 tracks' classes, in the ascending order of track quality. Both $n_{y1}$ e $n_{y2}$ are not dependent on the class, so they could be equal to 0,0233 cycles/m and 0,1312 cycles/m, respectively. However, the $A'$ constant depends on the track class as shown in Table 2.

*Table 2 - Roughness constant for each track class*

| **Track Class** | 6 | 5 | 4 | 3 | 2 | 1 |
|---|---|---|---|---|---|---|
| **A' [$10^{-7}$ m/cycle]** | 1,06 | 1,69 | 2,96 | 5,29 | 9,52 | 16,72 |

In addiction, it is possible to define the spectrum, $G_{w/r}(k_y)$, for an interval [$k_{y1}$, $k_{y2}$], taking in to account the relevant frequencies and the train velocity, dividing it in $N$ intervals, each one with width, $\Delta k_y$, and wave center, $k_y$. Therefore, is is obtained an artificial profile, $u_{w/r}(y)$, which is equal to the sum of co-sen functions with aleatory phase angles, $\theta_i$, in the interval [$0, 2\pi$], as follows:

$$u_{w/r}(y)=\sum_{i=1}^{n}\alpha_i \cos(k_{yi}\,y-\theta_i) \qquad \textit{Eq. 10}$$

where the $\alpha_i$ values are calculated making the area below the power spectrum, $G_{w/r}(k_y)$, for each interval, $\Delta k_{yi}$, with center, $k_{yi}$, to be equal to the square root of the artificial profile, $\alpha$.

$$\alpha_i=\sqrt{2G_{w/r}(k_{yi}\Delta k_y)} \qquad \textit{Eq. 11}$$

It is possible to do a time analysis instead of a spatial analysis, simply by changing the positions of the artificial profile, $u_{w/r}(y)$, by the instants when they happened, $u_{w/r}(t)$ (Illustration 1).

## Propagation of vibrations

The train traffic produces vibrations that spread, through its foundations, to large distances from the source. To better understand this behaviour we should remember the characteristics of the two main generated waves: volumetric and surface waves.

The first ones propagate in every direction, but the last ones only propagate superficially. Due to the fact that

geological materials are stiffer for compression loads, in each point at the surface, the first to arrive are compression waves, then shear waves and Love waves and, finally, Rayleigh waves.

Vibrations due to high-speed trains are considered to be confined to a small area, when compared to the shear wave length, so, Rayleigh waves are supposed to absorb most of the energy generated, because they have the smallest wave lengths.

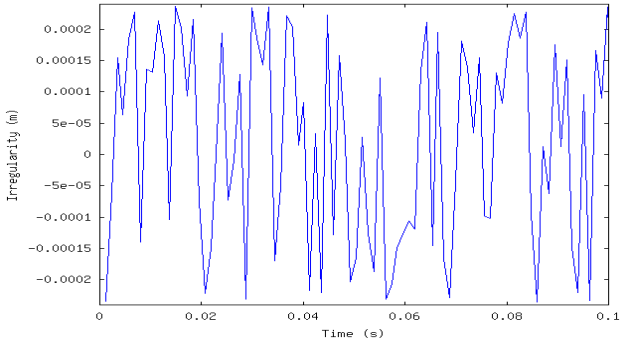


*Illustration 1 - Roughness values of the track*

## *Volumetric waves*

P-waves or compression waves' particles propagate with the same direction as the wave, with a speed of:

$$v_P^2 = \frac{E(1-\nu)}{\rho(1+\nu)(1-2\nu)} \qquad \textit{Eq. 1}$$

where $v_p$ stands for P-wave velocity, $E$ is the Young's Modulus, $\rho$ is the volume weight and $\nu$ represents the Poisson's ratio.

S-waves, also known as shear waves, have their particles moving transversely against the waves' direction of propagation, with a speed of:

$$v_s^2 = \frac{G}{\rho} \qquad \textit{Eq. 2}$$

where $v_S$ is the S-wave velocity and $G$ stands for the distortion modulus. Knowing the relation between the distortion modulus and Young's modulus, it is possible to write the next relation:

$$G = \frac{E}{2(1+\nu)} \qquad \textit{Eq. 3}$$

Therefore, the ratio between volumetric velocities is:

$$\frac{v_P}{v_S} = \sqrt{2\left(\frac{1-\nu}{1-2\nu}\right)} \qquad \textit{Eq. 4}$$

## *Surface waves*

The interaction between volumetric waves, the soil surface and its superior layers generate surface waves. They can be divided into two different types: Rayleigh and Love waves.

The first ones propagate with a cylindrical wave front and are the most important in terms of energy, due to

the smaller wave length. On the other side, there are the Love waves, which have its origin in the surface, when the top layer has a low shear velocity.

Therefore, the velocity of Love waves varies from shear wave velocity, in a low frequency half-space, $v_{S2}$, to shear wave velocity, in a high frequency half-space, $v_{S1}$.

$$\tan\left(2\pi f\sqrt{\frac{1}{v_{S1}^2}-\frac{1}{v_L^2}}\right)=\frac{v_{S2}^2\rho_2\sqrt{\frac{1}{v_L^2}-\frac{1}{v_{S2}^2}}}{v_{S1}^2\rho_1\sqrt{\frac{1}{v_{S1}^2}-\frac{1}{v_L^2}}} \qquad \textit{Eq. 5}$$

### *Damping*

In the propagation of vibrations there are two important types of damping: geometric and material (Kim & Lee, 2000).

## Geometric damping

Geometric damping is very important hence it is present in both volumetric and surface waves.

In 1904, Lamb studied the wave damping in elastic space and concluded that, in the case of an elastic space without material damping, the decrease in the wave amplitude was:

$$v=v_1\left(\frac{r_1}{r}\right)^m \qquad \textit{Eq. 6}$$

where $v$ is the peak particle velocity at a distance, $r$, from the source, $v_1$ is the peak particle velocity at a distance, $r_1$, from the source, and $m$ is a constant value as defined in Table 3.

*Table 3 - Values of "m" for various types of waves and loads applied to the surface of an elastic half-space, based on Hall (2002)*

| Wave Path | Source | Wave type | m |
|---|---|---|---|
| Surface | Point | Body wave | 2 |
| Surface | Point | Surface wave | 0,5 |
| Interior | Point | Body wave | 1 |
| Surface | Infinite line | Body wave | 1 |
| Surface | Infinite line | Surface wave | 0 |
| Interior | Infinite line | Body wave | 0,5 |

## Material damping

Bornitz (1931) stated that the material damping is defined as $e^{[-\alpha(r-r_1)]}$. Therefore, it is possible to determine the damping due to material and geometric damping simply by applying Eq. 7:

$$v = v_1 \left(\frac{r_1}{r}\right)^m e^{[-\alpha(r-r_1)]} \qquad \textit{Eq. 7}$$

where $\alpha$ is the coefficient of attenuation, which is representative of the frictional damping. Referring to different types of soil and vibration frequencies, it is possible to determine that coefficient using the following equation (Barkan, 1962):

$$\alpha_i = \frac{2\pi f \xi}{v_i} \qquad \textit{Eq. 8}$$

where $x$ is the damping ratio, $f$ stands for the vibration frequency and $v_i$ represents the wave propagation velocity.

## Bi-dimensional FE model

### *Numerical results vs "in situ" results*

In this work it had been used a two-dimension numerical model, but, because the phenomenon is three-dimensional, some measures had been taken to improve the final results.

There are some pros and cons when using a two-dimensional model. It represents only infinite train tracks, which is true in straight tracks, but it is impossible to module the sleeper passage. Instead of being a discrete medium, it becomes a continuous medium and, therefore, this should be taken into account when analysing the results. Another con is related to loading, in reality the axle loads are point loads, but in a two-dimensional model, those loads are line loads.

To evaluate the numerical model, some *in situ* tests had been considered. They were taken in Belgium, with the Thalys HST train at a speed of 314 km/h, and the experiment was performed by using 14 accelerometers, displayed perpendicularly to the track, at different distances, Illustration 2.

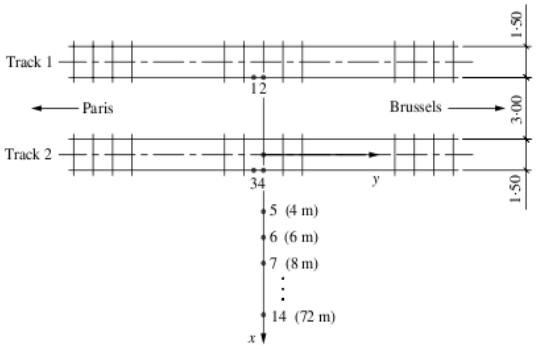


*Illustration 2 - Location of the accelerometers used in the experiment by Degrande & Schillemans (2001)*

The geometry and the characteristics of the site were taken into account in the numerical model, but, instead of 14 points, one by each accelerometer, it had been used only 12, due to the size of the model. The 2 missing points were the ones located further from the track.

The loading used in the model was divided in two parts: one referring to the axle loads of the Thalys HST

train and another referring to the wheel-track irregularities. To represent the latter, equivalent loads had been applied instead of induced displacements. Therefore, the load applied to the model was a sum of the axle loads and the track irregularities.

In the analysis of the results (*in situ* and numerical), in order to obtain the velocities and the displacements from the accelerations' values, it had been used a moving average filter of 100 points. This filter had been chosen mainly because is the easiest digital filter to apply and understand and is the optimal filter for reducing random noise, while retaining a sharp step response.

After analysing the first numerical results, it had became clear that some changes should be made to improve them. Therefore, taking into account that the numerical model is two-dimensional and the propagation phenomenon is three-dimensional, it was necessary to consider the geometrical damping in the model. The solution was to test three different correction factors, related to wave damping for point loads and line loads (Table 3): $1/\sqrt{r}$ , $1/r$ and $1/r^2$ , being *r* the distance to the source. After analysing the new values it was decided to compare only two alternatives: $1/\sqrt{r}$ and $1/r$ , because they gave the best results and were quite similar.

In Illustration 3 is presented a comparison between the corrected numerical results, by multiplying the original values by $1/\sqrt{r}$ and $1/r$ , and *in situ* results. It had been chosen 4 reference points for this analysis: two near the track (point 1 and 3) and two in the soil, one close and another further from the source (point 6 e 12).

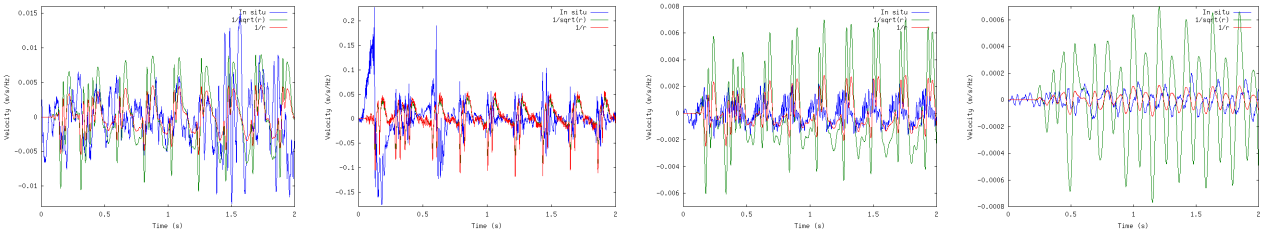

*Illustration 3 - Comparison of results of velocities between "in situ" results and numerical values corrected by* $1/\sqrt{r}$ *and* $1/r$ *. a) point 1; b) point 3; c) point 6; d) point 12.*

It is possible to see a total agreement, referring to time display, between maximums and minimums in the *in situ* results and numerical results. Furthermore, their amplitude is almost the same, for points near the track (point 1, 3 and 6), but, when moving away of the source (point 12), the results differ. The numerical results tend to have higher values than *in situ* ones (three and four times more sometimes), showing that damping tend to be higher in reality. However, the values corrected by $1/r$ tend to have better results.

In Illustration 4, it had been used a one third octave band analysis, which has been already adopted by some authors for the same purpose: Ju & Lin (2004), Degrande et al. (2006) and Thompson & Jones (2000). It is possible to register that the low frequency component (less than 4 Hz) becomes less important with increasing distances to the source. In the other hand, the high frequency component (more than 4 Hz) tends to increase with distance. Furthermore, for frequencies less than 4 Hz, there are major differences between

*in situ* and numerical results at shorter distances (point 1 and 3), but when frequencies increase, these differences tend to decrease and sometimes results become coincident. At large distances (points 6 and 12), some numerical results are greater than the *in situ* results (specially frequencies higher than 4 Hz and with the factor $1/\sqrt{r}$ ). In this analysis there are some maximums at 4, 10 and 20 Hz (point 1, 3 and 6) in the numerical results, but those aren't clear in the *in situ* ones. In point 12, 4 and 20 Hz maximums remain, but the 20 Hz has the bigger value (instead of the 4 Hz for the other points) due to the greater soil damping at low frequencies.

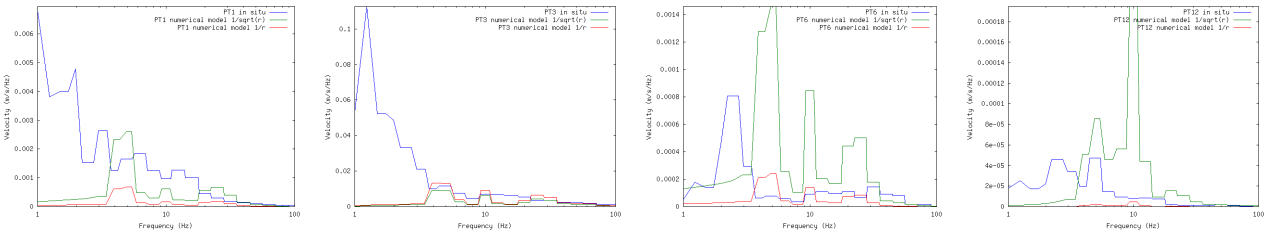


*Illustration 4- Comparison of results of velocities between "in situ" results and numerical values corrected by* $1/\sqrt{r}$ *and* $1/r$ *. a) point 1; b) point 3; c) point 6; d) point 12.*

To check which correction gives the better results has been made a comparison between *RMS* values and the distance to the source (Illustration 5), both for *in situ* and numerical results. The best results tend to be the ones corrected by the factor $1/r$ , which are almost coincident with some *in situ* values.

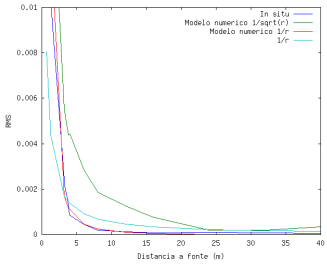


*Illustration 5 - "In situ" RMS values vs numerical RMS values, corrected by* $1/\sqrt{r}$ *and* $1/r$ *vs theoretical values*

## Conclusions

The additional consideration of irregularities in rail traffic vibrations tend to improve results, furthermore, both irregularities and axle loads are the most important actions in a passage of a train.

Two-dimensional models have some limitations, specially in terms of geometry and applied loads, however, they are easier and lighter to implement. In this work it has been shown that, making some corrections, it is possible to have almost the same results as a three-dimensional one.

Soil damping tend to decrease the low frequency component, with distance to the source more, than the high frequency component. This damping is far more relevant in the *in situ* results than numerical ones.

## References

**Barkan, D. (1962)**, "Dynamic of Bases and Foundations", McGraw-Hill.

**Bornitz, G. (1931)**, "Über die Ausbreitung der von Groszkolbenmashinen Erzeugten Bodenschwingen in die Tiefe, Springler, Berlin, Germany.

**Degrande, G., Schevenelsa, M., Chatterjeea, P., Veldea, W., Hölscherb, P., Hopmanb, V., Wangc, A., Dadkahd, N. (2006)**, "Vibrations due to a test train at variable speeds in a deep bored tunnel embedded in London clay". Journal of Sound and Vibration, vol. 293, ed. 3-5, pp. 626-644.

**Degrande, G., Schillemans, L. (2001)**, “Free field vibrations during the passage of a Thalys high-speed train at a variable speed”. Journal of Sound and Vibration, vol. 247, ed. 1, pp. 131-144.

**Esveld, C. (2001)**, “Modern Railway Track”, MRT-Productions.

**Gupta, S., Liu, W., Degrande, G., Lombaert G., Liu, W. (2007)**, “Prediction of vibrations induced by underground railway traffic in Beijing”. Journal of sound and vibration, vol. 310, ed. 3, pp. 608-630.

**Hall, L. (2002)**, “Simulations and analyses of train-induced ground vibrations in finite element models”. Soil Dynamics and Earthquake Engineering, vol. 23, ed. 5, pp. 403-413.

**Ju, S., Lin, H. (2004)**, "Analysis of train-induced vibrations and vibration reduction schemes above and below critical Rayleigh speeds by finite element method". Soil Dynamics and Earthquake Engineering, vol. 24, ed. 12, pp. 993-1002 .

**Kenney (1954)**, “Steady-state vibrations of a beam on elastic foundation for moving load”. Journal of Applied Mechanics, vol. 21, ed. 4, pp. 359-364.

**Kim, D., Lee, J. (2000)**, “Propagation and attenuation characteristics of various ground vibrations”. Soi Dynamics and Earthquake Engineering, vol. 19, ed. 2, pp. 115-126.

**Nielsen, J. (2008)**, “High-frequency vertical wheel–rail contact forces. Validation of a prediction model by field testing”. Wear, vol. 265, ed. 9-10, pp. 1465-1471.

**Sheng, X., Jones, C., Thompson D. (2003)**, “A theoretical model for ground vibration from trains generated by vertical track irregularities”. Journal of Sound and Vibration, vol. 272, ed. 3-5, pp. 937-965.

**Thompson, D., Jones, C. (2000)**, A Review of the Modelling of Wheel Rail Noise Generation". Journal of Sound and Vibration, vol. 231, ed. 3, pp. 519-536.